

Modeling and Characterization of Superconducting MEMS for Microwave Applications in Radioastronomy

N. Al Cheikh^{*1}, P. Xavier¹, J.-M. Duchamp¹, K. Schuster²

¹Institute of Microelectronics, Electromagnetism and Photonics (IMEP-LAHC) – Grenoble (France),

²Institute of Millimetrics Radio Astronomy (IRAM) – Grenoble (France)

^{*}IMEP-LAHC - Minatec - INPG 3 Parvis Louis Néel - BP 257, 38016 Grenoble Cedex 1, alcheikh@minatec.inpg.fr

Abstract: Superconducting GHz electronics circuits are frequently used in Radio Astronomy instrumentation. The features of these instrumentations can be significantly improved by using tuneable capacitances, which can be realized by electrically actuated, micromechanical bridges (MEMS) made of superconducting Niobium (Nb). In order to analyse the electromechanical behaviour of such devices and the intrinsic stress gradient induced during the fabrication process, COMSOL simulations of the bridges have been performed. The simulations are in agreement with the theoretical approach and are experimentally validated.

Keywords: tuneable capacitances, microwave, superconductor, MEMS, radioastronomy.

1. Introduction

Superconducting electronic components are widely used in the field of radio astronomy, because of their low noise and loss performances. Furthermore, Superconductor-Insulator-Superconductor (SIS) mixers are implemented in much radio astronomy instrumentation due to their high sensitivity.

Nevertheless, some transmitter's signals such as radars and satellites can perturb broadband astronomical signal and saturate SIS mixers because of their high amplitude [1].

A solution to this problem is based on a narrow frequency band detection swept on the entire observed band (between 72GHz and 115GHz at the IRAM).

For this purpose, variable tuning elements are of increasing interest. Tuneable capacitances, so-called varactors, represent one important class of tuneable circuit elements. They are widely applied in wireless communication or radars, where they act as basic elements for adjusting the operation range of variable filters, phase shifters or transceivers.

New devices manufactured with superconducting materials meet these demands

and are well established in this field [2]. These variable devices based on capacitive MEMS were fabricated by the IRAM which is interested in using these components for agile impedance matching networks and filters [3]-[4].

The bridges are actuated by applying a suitable voltage between the bridge and the ground electrode underneath (figure 1).

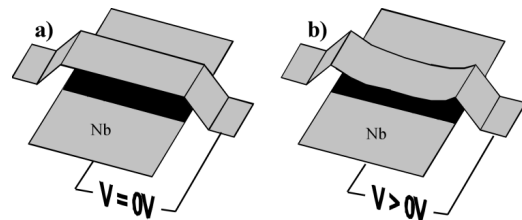


Figure 1. Schematic picture of an air bridge with electrode underneath for electrostatic actuation a) without and b) with applied voltage.

This paper presents how to describe a 2D MEMS taking into account coupled electrostatics and mechanics problems.

This study is only the first part of a regional project SupraMEMS. The final goal of the project is to propose a multiphysics model (electromechanical, microwave and superconducting) of these tuneable capacitances.

In the first section, the MEMS fabrication process is described.

In the second one, measurements of capacitance value versus the voltage characteristic $C(V)$ are compared with a simple capacitance model. The assumption of a bending effect of the bridge layer is proposed.

A more accurate model is proposed in the third section to extract the new capacitance value versus the voltage characteristic $C(V)$ and the new pull in voltage V_{PI} .

Then this model is confirmed by COMSOL simulations in section four. In this section, the slope edge variation is also taken into account.

Finally this paper draws out conclusions on the bending effect of the air bridge on the MEMS capacitance feature.

2. Fabrication process

For decade now, many superconducting electronic circuits are based on Niobium (Nb) with a critical temperature of 9°K. The fabrication process of IRAM MEMS is described on figure 2a.

A Nb transmission line is realized in the first step. Then a photoresist polymer AR-4000/8 (ALLRESIST GmbH) is used as a sacrificial layer. This layer has a thickness about 5 μm. Smooth rims of the sacrificial resist layer are necessary to avoid breaking of the Nb film at side edge of the MEMS. To obtain sufficiently smooth edges, the AR-4000/8 was baked in a convection oven before exposure and after development.

The Nb layer was sputtered, in the third step, by DC-magnetron sputtering in steps of 9 s deposition and 5 min break (figure 2b). The break delays are needed to reduce surface heating and thus deformation or polymerization of AR-4000/8 layer.

The widths of the bridges are defined in this step by a negative tone photoresist mask. For a good coverage of the structures, the same thick resist AR 4000/8 with a reversal process is used. Through this resist mask, which covers the surface of the Nb bridges, the no-covered parts were etched by RIE (Reactive Ion Etching) as shown in figure 2c.

The final step wash away the sacrificial layer in hot acetone at 70°C (figure 2d).

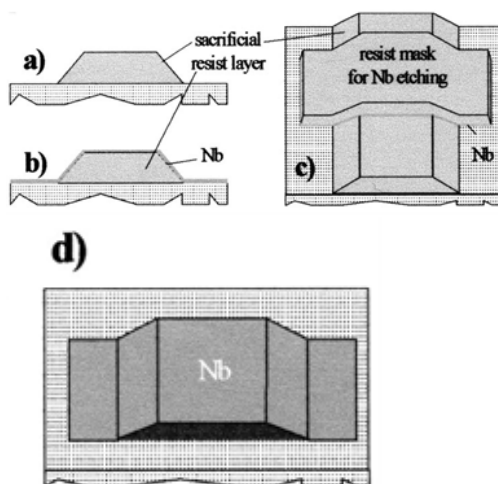


Figure 2. Schematic of the fabrication process for sputtered Nb air bridges.

3. First experimental observation

Two sizes of MEMS are designed. The first one has 5 μm high, 100 μm long, 100 μm wide, but the capacitive part has only 90 μm long. This MEMS capacitance topology is closed to the plane capacitance one (figure 3). So a first approximation of the capacitance can be obtained with the simple equation (1)

$$C(0) = \frac{\epsilon_0 \cdot W \cdot L}{g_0} \quad (1)$$

g_0 is the height of the bridge, W the width and L the length. ϵ_0 is the air permittivity equal to $8,85 \cdot 10^{-12}$ F/m.

For the first size; MEMS should have a capacitance value $C(0)$ about 16 fF. The second MEMS size is 4 μm high, 60 μm long, 100 μm wide. In this case $C(0)$ is near 13.3 fF.

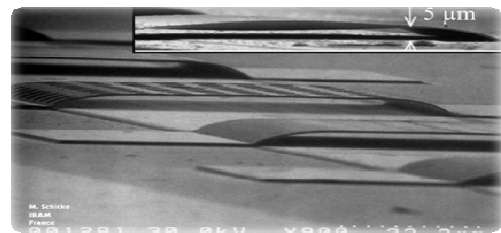


Figure 3. Picture of an air bridge with electrode underneath for electrostatic actuation. The inset shows the bending of the bridge layer and the reduced height due to stress in the Nb film.

Capacitance-voltage measurements are shown on figure 4. We can noticed that $C(0)$ values are between 30.4 fF and 33.4 fF, two times greater than the expected values.

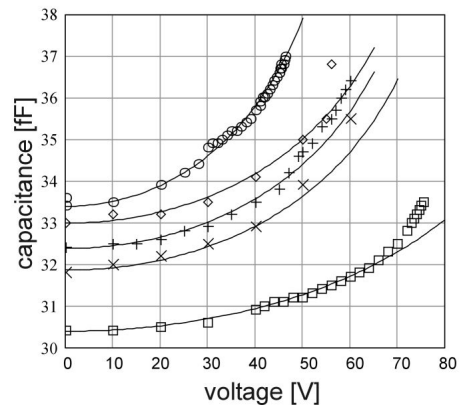


Figure 4. Measured capacitance-voltage for various MEMS.

Of course, there are some uncertainties on the MEMS length and width during the process and edge effect are not taking into account in equation (1) but these errors can not justify a 100 % error on C_0 value.

We assume that the only parameter able to explain this difference is the height of the air bridge. It should be smaller than expected at the middle of the MEMS length. It is probably due to the bending of the bridge layer after removing the sacrificial layer and releasing the MEMS (figure 3 insert).

This effect could have two causes. First; a lengthening ΔL can be caused by a tensile stress and shrinking of the sacrificial layer during deposition and cooling time. Second; a variation of MEMS side slope could occur when the bridge is released.

4. Theoretical beam modelling

In this section, we present a new electromechanical model of these devices. This model takes into account technological imperfections such as the bending of the bridge. This theoretical study of the air bridge shape gives new values for $C(V)$ and the pull in voltage V_{PI} .

4.1 New $C(0)$ equation

We assume that the bending bridge is a Fixed-Fixed beam with a length equal to $L + \Delta L$. The height of the bridge along the length of the MEMS can be described by a cosine equation.

$$y(x) = \frac{y_{max}}{2} \left(1 - \cos\left(\frac{2\pi x}{L}\right) \right) \quad (2)$$

y_{max} is the maximal difference between the expected height and the height with bending in the middle of the MEMS.

The new capacitance equation becomes

$$C(0) = \int_0^L \frac{\epsilon_0 W}{g_0 - y(x)} dx \quad (3)$$

If these capacities can be described as the sum of elementary plane capacitance, integration result is.

$$C_0 = \frac{\epsilon_0 WL}{g_0 \sqrt{1 - \frac{y_{max}}{g_0}}} \quad (4)$$

With this new expression for $C(0)$, the largest of the bending of the bridge, obtained for 33.4 fF

(figure 4), must be between 71% to 75% of the height. The gap variation is between 3.6 μm and 3.8 μm .

4.2 Energetical approach

In this sub-section, we describe the variation of the voltage $V(y_{max})$ when we took into account an energetical approach where the equations of the device electrostatic energy and of the mechanical energy are equalled.

The expression of mechanical energy is given by the theorem of *Clapeyron* [7] :

$$U_m = \frac{1}{2} \int_v \sigma \epsilon dV \quad (3)$$

Where $\sigma = \pi^2 E (y_{max}')^2 / 4 L^2$ is an estimated value of the induced axial stress [8], dV is the volume variation, y_{max}' is the maximal buckling in the middle after application of the voltage and E is the young modulus.

$\epsilon = \pi^2 (y_{max}' - y_{max})^2 / 4 L^2$ is the strain of the beam [6].

Thus, in Equation (3), the expression of the mechanical energy becomes:

$$U_m = \pi^4 E W h y_{max}'^2 (y_{max}' - y_{max})^2 / 32 L^2 \quad (4)$$

where h is the thickness of the beam.

The expression of the electrostatic energy is given by :

$$U_e = \frac{1}{2} C V^2 \quad (5)$$

The expression of the capacitance C is the same as $C(0)$ when y_{max} is replaced by y_{max}' because the profile is still assumed to be of cosine shape before and during the application of the voltage. So the expression of $C(y_{max}')$ is:

$$C = \frac{\epsilon_0 WL}{g \sqrt{1 - \frac{y_{max}'}{g}}} \quad (6)$$

Finally, the equation (4) is balanced with equation (5) to find the expression of the voltage variation $V(y_{max}')$:

$$V = \sqrt{\frac{g \sqrt{1 - \frac{y_{max'}}{g}} \pi^4 E h y_{max'}^2 (y_{max'} - y_{max})^2}{16 L^4 \epsilon_0 W}} \quad (7)$$

The pull-in voltage V_{PI} can be derived when the variation of the voltage $V(y_{max'})$ is plotted. The maximum of the curve is the value of V_{PI} ; for example, on the curve having $C(0)=33\text{fF}$, the deduced value of V_{PI} is 88.39 V (Figure 5).

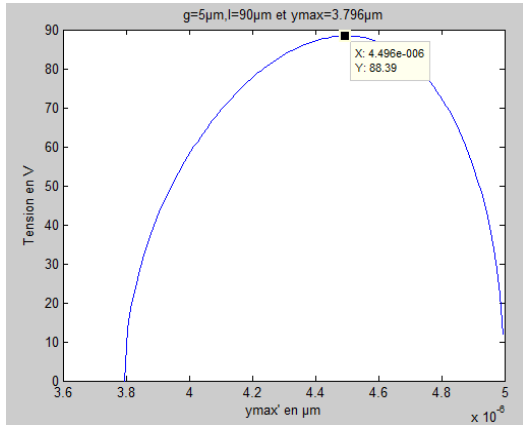


Figure 5. Schematic of the $V(y_{max'})$ variation, the maximum show the voltage V_{PI} equal to 88.39 V.

Besides the calculated curves of $C(V)$ follow easily using the values of $y_{max'}$ which has come from $V(y_{max'})$ in the expression of $C(y_{max'})$ (Figure 6).

These curves are very close to the ones experimentally obtained. These results validate the COMSOL modeling of the superconducting MEMS.

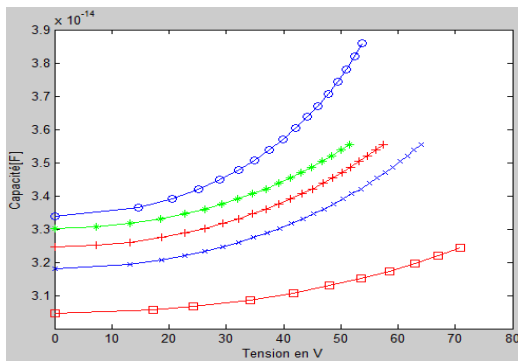


Figure 6. Theoretical Voltage dependence of the capacitance for different air bridges. These curves are calculated taking the parameters in the Tab 1.

Symbol	$g(\mu m)$	$y_{max}(\mu m)$	$h(nm)$	$L(\mu m)$
O	4	3.367	410	60
□	4	3.24	160	60
X	5	3.746	240	90
+	5	3.796	240	90
*	5	3.836	240	90

Tab1: the height of the MEMS is given by g and in the centre by $(g - y_{max})$, where $(g - y_{max})$ is the height when $V = 0$ (initial deflection).

5. COMSOL Multiphysics beam simulations

To confirm these previous theoretical results of the bending beam, simulations with COMSOL have been done.

This section describes the different steps necessary to simulate correctly the IRAM MEMS in COMSOL Multiphysics.

5.1 $C(0)$ simulation

In the first step, to find the values of the capacitance $C(0)$, the method consists in applying a force on the free boundary (figure 7) of a no-buckling beam in order to create a buckling. Then the schema of the simulated buckling beam will be extracted (figure 8).

In this new schema, the electrostatical domain is applied to find $C(0)$. In this context, a 2D simulation is used in the Model Navigator; from the COMSOL MemS Module, the Structural Mechanics is used for Plane stress and from The COMSOL Multiphysics Module the Deformed Mesh, where the COMSOL Multiphysics translates the application-mode equations between the fixed and moving frames.

The program keeps pictures of the movements using the moving Mesh (ALE). After that, for the Modeling geometry, we draw a Fixed-Fixed beam soft buckling and soft board. In this way, we can put the necessary properties for plane stress and for Boundary Conditions. The first in the Subdomain setting concerned the values of young's modulus (E), Poisson's ratio (ν) and the thickness; the second lead to choice between the fixed beam and the free beam. When we can put a force on the Free beam, after every application of the force, we can find the value of y_{max} to know $C(y_{max})$.

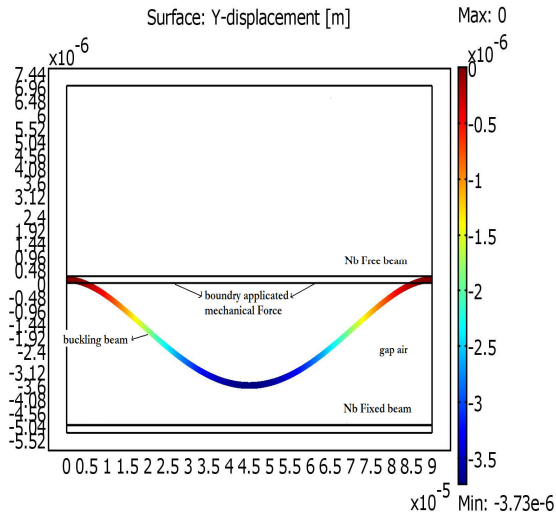


Figure 7. schematic of the application of mechanical Force on fixed-fixed beam.

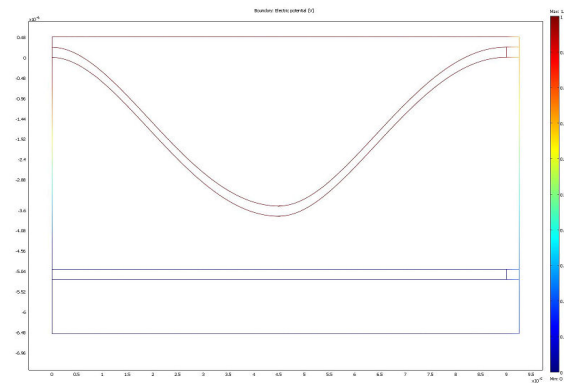


Figure 8. Extrude the schema of figure 7 where the created Geometry From Mesh is used

The second step consists in extruding the schema of the buckling beam after the application of a force (figure 8); we can use for that in COMSOL Mesh the “Create Geometry From Mesh”.

The third step consists in using the electrostatic in the Mems Module, use the “Electrostatics application mode” which solves the electric potential (see figure 9). Now $C(0)$ can be calculated from the stored electric energy in the capacitance, W_e , and the voltage across the capacitor:

$$C(0) = 2W_e / \Delta V^2$$

Same steps are done for the beam with the supports where we put the condition “fixed boundary” on the board and the Force is only applied on the Free beam (Figure 10).

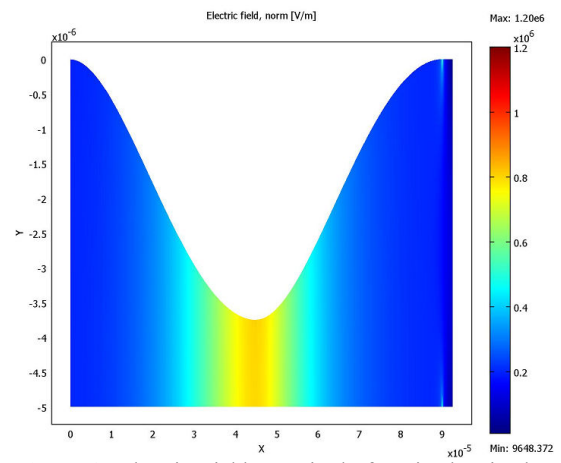


Figure 9. Electric Field magnitude for Fixed –Fixed beam.

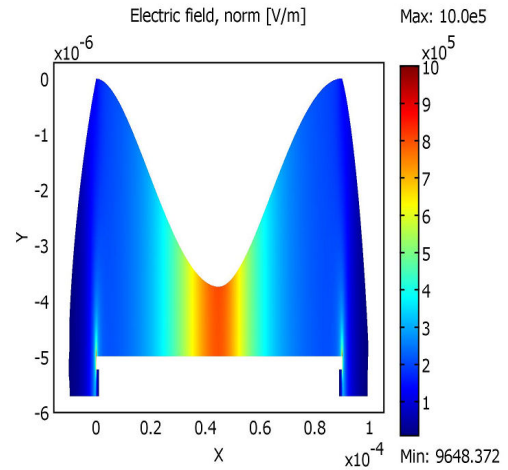


Figure 10. Electric Field magnitude for beam with supports.

5.2 $C(V)$ and V_{pi} Simulations

To calculate $C(V)$ a coupling between mechanical and electrostatic is necessary. The first step consists in taking into account the extrude schema of Mems when the plain stress, Moving Mesh and Electrostatics are applied in the COMSOL simulation. Here electrostatic forces named $F_{es_nTx_emes}$ and $F_{es_nTy_emes}$ are automatically generated variables from the Electrostatics application mode($emes$) and define the x- and y- components of the electrostatic force which are used in place of the mechanical force for the coupling Electrostatics –Mechanics and for the boundary condition for electrostatics (figure 11) when we put V_{in} in the V_0 Boundary.

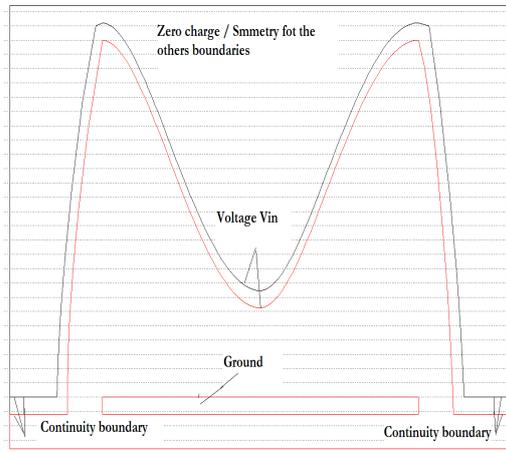


Figure 11. Boundary condition of the Mems by the coupling Electrostatics-Mechanics used with Mesh(ALE)

In this coupling, the values of the capacitances cannot be calculated; only the variation of the place of the free beam (Figure 12) and the voltage V_{pi} .

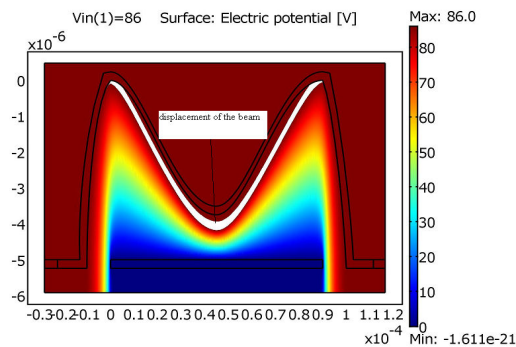


Figure 12. Surface Electric potential, the white color represents the displacement y after the coupling Electrostatics-Mechanics

In fact, then during the simulation an error message (“Failed to find a solution for all parameters, even when using the minimum parameter step.”) appears, this indicates that the pull-in voltage has been reached.

To find $C(V)$, the schema of figure 12 is extruded to a new schema after every application of the voltage because it is needed to apply the same steps as in the paragraph 5.1 to calculate the capacitance of Figure 13. A good agreement between measures, theory and simulations is observed.

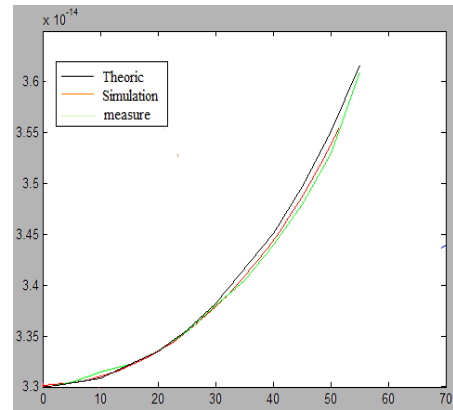


Figure 13. Comparison between measures, theory and simulations of the Mems with the support

6. Conclusions

In this paper, the necessary steps to simulate particular MEMS used in radioastronomy applications on COMSOL Multiphysics are described. The obtained $C(V)$ results are validated from experimental capacitance measurements and theoretical calculations.

7. References

1. K.H. Gundlach and M. Schicke, Supercond. Sci Technol, 13, R171, 2000
2. J. Zmuidzinas and P.L. Richards, Proc, IEEE, 92(10), 1597, 2004
3. J. Yao, J. Micromech Microeng, 10, R9, 2000
4. R. Borwick, P. Stupar, J.F. DeNatale, R. Anderson, R. Erlandson, IEEE Trans Microwave Theory and Techniques, 51(1), 315, 2003
5. H. Guckel, T. Randazzo, D.W. Burns, A Simple Technique for the determination of mechanical Strain in Thin Films with Applications to Polysilicon, 15/11/1984.
6. W.Fang and J.A.Wickert, Post Buckling of Micromechined beams, J.Micromech Microeng, 116-112, 4 August 1994.
7. F. Fey, Analyse des structures et milieu continus, Mecanique des structures, Page 237.
8. S. Pamidighantam, R. Puers, K. Baert and H.C. Tilmans, J.Micromech Microeng, 458-464, June 2002.

8. Acknowledgements

This work has been funded from the French Rhone Alpes Region, in the frame of the SUPRAMEMS project (MicroNano cluster) and in cooperation with the partners IN Lyon, Ecole des Mines de St Etienne and Infiniscale.